Localized two-dimensional shift correlated MR spectroscopy of human brain

ARTICLE *in* MAGNETIC RESONANCE IN MEDICINE · JULY 2001

Impact Factor: 3.57 · DOI: 10.1002/mrm.1160 · Source: PubMed

11 AUTHORS, INCLUDING:

Michael Albert Thomas
University of California, Los Angeles
181 PUBLICATIONS **2,600** CITATIONS
SEE PROFILE

John G Curran
Phoenix Children's Hospital
57 PUBLICATIONS **1,814** CITATIONS
SEE PROFILE

Magnetic Resonance in Medicine 46:58–67 (2001)

Localized Two-Dimensional Shift Correlated MR Spectroscopy of Human Brain

M. Albert Thomas,[1,2*] Kenneth Yue,[1] Nader Binesh,[1] Pablo Davanzo,[2] Anand Kumar,[2] Benjamin Siegel,[2] Mark Frye,[2] John Curran,[1] Robert Lufkin,[1] Paul Martin,[3] and Barry Guze[1,2]

A two-dimensional (2D) chemical shift correlated MR spectroscopic (COSY) sequence integrated into a new volume localization technique (90°–180°–90°) is proposed for whole-body MR spectroscopy (MRS). Using the product operator formalism, a theoretical calculation of the volume localization as well as the coherence transfer efficiencies in 2D MRS is presented. Phantom model solutions were used to test and optimize the efficiency of the proposed sequence. A combination of different MRI transmit/receive RF coils was used: a head MRI coil and a 3″ surface coil receive combined with a body coil transmit. The J cross-peaks due to N-acetyl aspartate (NAA), glutamate/glutamine (Glx), myo-inositol (mI), creatine (Cr), choline (Ch), aspartate (Asp), γ-aminobutyrate (GABA), taurine (Tau), glutathione (GSH), threonine (Thr), and macromolecules (MM) were identified. The cross-peak intensities excited by the proposed 2D sequence were asymmetric with respect to the diagonal peaks. Localized COSY (L-COSY) spectra of cerebral prefrontal and occipital gray/white matter regions in 15 healthy controls are presented. Magn Reson Med 46:58–67, 2001.

Key words: localized two-dimensional COSY; human brain; ^{1}H MR spectroscopy

Due to the recent improvements in the design of B_0 gradient and RF coils, ^{1}H MR spectra have been recorded in human brain with excellent water suppression using short TE, as short as 15 ms, and several cerebral metabolites have been identified (1–4). During the past decade alterations in several metabolites, namely, N-acetylaspartate (NAA), glutamate/glutamine (Glx), choline (Ch), creatine (Cr), myo-inositol (mI), and γ-aminobutyrate (GABA) have been reported in different pathologic states involving the central nervous system (CNS) (5–10). Absolute quantitation of cerebral metabolites in vivo has also been reported for only a few metabolites, albeit with limited success (11–13). Due to severe overlap of these metabolites, an unambiguous assignment of J-coupled metabolite multiplets is severely hindered at 1.5 T field strength.

One-dimensional (1D) MR spectral editing techniques to unravel the overlapping resonances rely on J-coupled proton metabolites that have well-separated multiplets. A technique based on subtraction methodology is very sensitive to motion artifacts leading to subtraction errors. An additional drawback is that only one metabolite can be identified at a time. Successful attempts in editing GABA and glutamate using whole-body MRI/MRS scanners have been presented by other researchers (13,14). Single-shot-based multiple-quantum filtered MR spectroscopic sequences have also been implemented on whole-body scanners, but a severe signal loss associated with various coherence transfer pathways made it less attractive to human applications (15–17).

A localized version of a two-dimensional (2D) J-resolved MR spectroscopic (JPRESS) sequence using the PRESS sequence for volume localization was recently proposed (18–20). Even though the JPRESS sequence retains 100% of the magnetization from a localized volume of interest (VOI), the strong coupling effect inherent at 1.5 T field strength resulted in a complex 2D cross-peak pattern for NAA, glutamate/glutamine, GABA, and other cerebral metabolites (19). Also, some of the 2D cross-peaks were heavily T_2-weighted during the long incremental delays necessitated by the second dimension of the JPRESS spectrum. An oversampled J-resolved sequence has also been proposed recently (21).

Compared to the 2D J-resolved spectra, a COSY spectrum produces a better dispersion of J-cross-peaks, although it requires a larger spectral window to be sampled during the evolution period (22). Different versions of the localized COSY sequence have been implemented by other researchers (23–33). McKinnon and Bosiger (23) proposed a conventional COSY sequence with hard RF pulses (90°–t_1–90°) followed by three volume selective 180° RF pulses. Haase et al. (24) implemented a COSY combined with an outer volume suppressing sequence, namely, LOCUS. Many previous attempts to develop localized 2D COSY spectra yielded only the phantom results (23–26) or rat brain spectra using a surface coil without a built-in localization sequence (27). A new gradient enhanced COSY in combination with VOSY used the STEAM sequence for volume localization (30). A human brain 2D COSY spectrum using a 2 T MRI scanner was recorded in a large occipital voxel (30). Homonuclear decoupled in vivo ^{1}H MR spectra using constant time chemical shift encoding were presented by Dreher and Leibfritz (31). Nonlocalized versions of COSY spectra have also been recorded in rat brain and rabbit kidney by other researchers using the high field NMR spectrometers (32,33).

[1]Department of Radiological Sciences, University of California, Los Angeles, California.

[2]Department of Psychiatry, University of California, Los Angeles, California.

[3]Department of Hepatology, University of California, Los Angeles, California.

Presented at the 40th ENC Meeting, Orlando, Florida, March 1–5, 1999, and the 8th ISMRM Meeting, Denver, Colorado, April 1–7, 2000.

Grant sponsor: National Institute of Mental Health; Grant number: MH-58284; Grant sponsors: Stanley Foundation; Wendy Will Case Cancer Foundation; Whitaker Foundation.

*Correspondence to: M. Albert Thomas, Ph.D., Radiological Sciences, Box #951721, UCLA School of Medicine, 10833 Le Conte Avenue, Los Angeles, CA 90095-1721. E-mail: athomas@mednet.ucla.edu

Received 20 March 2000; revised 20 December 2000; accepted 9 February 2001.

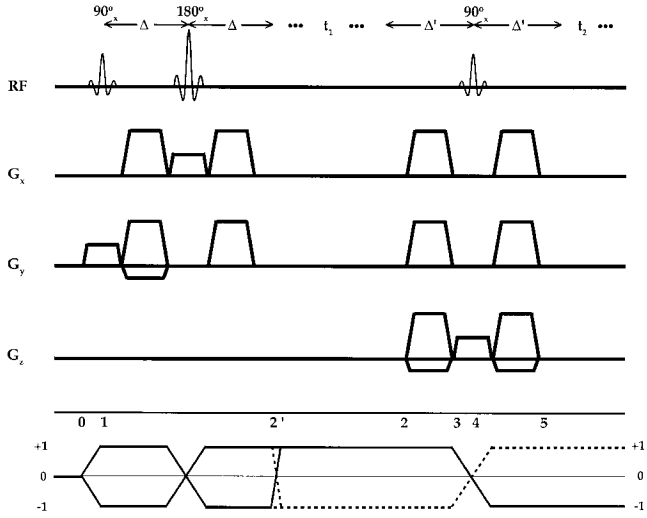

FIG. 1. Localized two-dimensional shift correlated MR spectroscopic sequence (L-COSY). The RF pulse scheme consisted of three RF pulses (90°, 180°, 90°) which were slice-selective along three orthogonal axes. A pair of B_0 gradient crusher pulses were symmetric with respect to the slice-refocusing 180° RF pulse. The last slice-selective 90° RF pulse with a pair of symmetric B_0 gradient crushers also served as a coherence transfer pulse for the L-COSY spectrum. The coherence transfer pathway diagram depicts the different stages of conversion of magnetization/coherences (22).

Two major problems yet to be resolved in the localized 2D MR spectroscopy are: 1) minimizing the RF pulses used for both localization and coherence transfer, taking into consideration that some of the brain metabolites have short T_2; and 2) recording the localized 2D spectra of human organs in a reasonable time duration. The objectives of the current study were twofold: 1) to implement a new version of a localized 2D COSY sequence (L-COSY) and its 1D analog on a 1.5 T whole-body MRI/MRS scanner with a minimal number of RF pulses for volume localization and coherence transfer; and 2) to record L-COSY spectra in the prefrontal and occipital gray/white matter of healthy human brains.

MATERIALS AND METHODS

Pulse Sequence

Figure 1 depicts a Localized 2D COrrelated SpectroscopY (L-COSY) sequence with the pertinent coherence transfer pathway diagram. The VOI was localized in one shot by a combination of three slice-selective RF pulses (90°–180°–90°), a new MRS volume localization sequence called CABINET (Coherence trAnsfer Based spIN-Echo specTroscopy). The last slice-selective 90° RF pulse acted also as a coherence transfer pulse for the 2D spectrum. An incremental period for the second dimension was inserted immediately after the formation of the Hahn spin-echo. In addition to the slice-selective 180° RF pulse, there were refocusing B_0 gradient crusher pulses before and after the last 90° RF pulses, the action of which is justified in the theory section. A minimum number of eight averages was acquired for every incremental period in order to improve the signal-to-noise from a localized volume. The proposed sequence can be considered a single-shot technique in terms of volume localization and coherence transfer. However, there was also an 8-step phase cycling, two steps superimposed on each RF pulse in order to minimize the effect of the RF pulse imperfection. Each time point of the pulse sequence is marked as shown in Fig. 1 to evaluate the time course of magnetization that will take into account the rotation after each RF pulse and evolution during the B_0 gradient pulses and the incremental period.

MR Parameters

We used the numerically optimized Shinnar-Le Roux (SLR) RF pulses (34) with durations of 1.8, 5.2, and 1.8 ms, respectively. 2D L-COSY spectra were recorded using the following parameters: TR = 2 sec, minimal TE of 30 ms, 40, 64, 128, and 256 increments of Δt_1 and 8–16 number of excitations per Δt_1. The raw data was acquired using 1024–2048 complex points and the spectral window along the first dimension was 2500 Hz. Δt_1 was incremented to yield a spectral window of 625 Hz along the second dimension. A 1.5 T whole-body MRI/MRS scanner (GE Medical Systems, Waukesha, WI) with "echo-speed" gradients at a minimal rise time of 120 μs was used. The crusher gradient pulses for the 180° and the last 90° RF pulses used a maximum amplitude of 22 mT/m and the duration of each pulse was 4 ms long. A frequency offset of 128 Hz was included for the three slice-selective RF pulses to minimize the voxel shifts. The CABINET sequence was used for localized "shimming" process to improve the static field B_0 homogeneity over the voxel under consideration. Typical linewidth of water resonance was 9 Hz in brain voxels and 6 Hz in phantoms. Prior to the localization by the CABINET sequence, we used a CHESS sequence of three frequency-selective water suppression pulses with a bandwidth of approximately 75 Hz (11), each followed by the dephasing B_0 gradient pulses. A numerically optimized SLR waveform was used for each suppression RF pulse (34). A head MRI transmit/receive coil operating in the quadrature mode was used for in vitro measurements only. Otherwise, a 3″ surface receive coil was used for signal reception while the body RF coil was used for transmission in acquiring both MRI and MRS.

Brain Phantom

A GE brain MRS phantom (35), MRS-HD sphere (GE Medical Systems, Milwaukee, WI), was used to optimize the L-COSY and CABINET sequences. It consisted of the following chemicals: 1) N-acetyl-L-aspartic acid (NAA, 12.5 mM), 2) creatine hydrate (Cr, 10 mM), 3) choline chloride (Ch, 3 mM), 4) myo-inositol (mI, 7.5 mM), 5) L-glutamic acid (Glu, 12.5 mM), 6) DL-lactic acid (Lac, 5 mM), 7) sodium azide (0.1%), 8) potassium phosphate monobasic (KH_2PO_4, 50 mM), and 9) sodium hydroxide (NaOH, 56 mM). The phantom also contained 1 ml/l Gd-DPTA (Magnevist).

Human Subjects

Fifteen healthy volunteers (21–69 years old, mean = 33.8) have participated in this study so far. Consent was obtained from every participant in keeping with the requirements of the institutional review board (IRB).

Theory

We present here a theoretical analysis to calculate 1) the volume localization efficiency of the 1D MRS signal amplitude in a single spin ($I = 1/2$) system using the CABINET sequence, and 2) the amplitudes and phases of L-COSY diagonal and cross-peaks in a weakly coupled two spin ($I = 1/2$, $S = 1/2$) system. A product operator formalism was used to evaluate the time course of the magnetization (22).

In order to calculate the efficiency of volume localization with the proposed sequence, a single spin system (I) is considered first.

Efficiency of Volume Localization

Prior to the first slice-selective 90° RF pulse, the spin-state ($I = 1/2$) is represented by:

$$\sigma_0 \propto I_z. \qquad [1.1]$$

Immediately after the first 90° RF pulse along x-direction, the magnetization is rotated to the transverse plane characterized by:

$$\sigma_1 \propto -I_y. \qquad [1.2]$$

After an evolution during a train of a 180° refocusing RF pulse sandwiched by a pair of the B_0 crusher gradient pulses, formation of a spin-echo is ascertained by:

$$\sigma_2 \propto I_y. \qquad [1.3]$$

A second pair of B_0 gradient crusher pulses (durations of τ_1 and τ_2) is played around the last slice-selective 90° RF pulse. The spin state before the last 90° RF pulse rotation is:

$$\sigma_3 \propto I_y \cos\theta_1 - I_x \sin\theta_1 \qquad [1.4]$$

where

$$\theta_1 = 2\pi\gamma \int \Delta B_0 \, d\tau_1. \qquad [1.4a]$$

The last 90° RF pulse along x-direction will turn I_y into I_z, and I_x will remain unchanged.

$$\sigma_4 \propto I_z \cos\theta_1 - I_x \sin\theta_1. \qquad [1.5]$$

At this point, evolution of I_z will be excluded since there will be no observable signal. The spin state after an evolution during the last set of B_0 gradient crushers:

$$\sigma_5 \propto -I_x \cos\theta_2 \sin\theta_1 - I_y \sin\theta_2 \sin\theta_1 \qquad [1.6]$$

where

$$\theta_2 = 2\pi\gamma \int \Delta B_0 \, d\tau_2. \qquad [1.6a]$$

A static field gradient pulse of ΔB_0 and gyromagnetic ratio (γ) were used in Eqs. [1.4a] and [1.6a]. When the gradient crushers are balanced ($\theta_1 = \theta_2$) and using the identities:

$$\frac{1}{2\pi}\int_0^{2\pi} \cos\theta \sin\theta \, d\theta = 0 \quad \text{and} \quad \frac{1}{2\pi}\int_0^{2\pi} \sin^2\theta \, d\theta = \frac{1}{2} \qquad [1.7]$$

$$\sigma_5 \propto -I_y/2. \qquad [1.8]$$

In contrast to the commonly used PRESS sequence (90°–180°–180°) with 100% efficiency, the CABINET sequence retains only 50% net signal from the localized volume due to a selection of only N-type echo enabled by the B_0 gradient crusher pulses (22). A 50% efficiency of the CABINET sequence was confirmed with the simulated 1D spectra of selected metabolites using GAMMA library (36). While using the inhomogeneous RF pulses delivered by a surface coil or other types, one has to consider the influence of flip-angle errors. In the CABINET sequence with the flip-angle distribution of ($\varphi°$,2$\varphi°$,φ0), the total signal amplitude from the VOI will be scaled by a factor of sin4φ. The maximum attenuation coefficient for the PRESS sequence ($\varphi°$,2φ0,2φ0) will be sin5φ.

2D MR Signal Acquired by L-COSY

The amplitude and phase characteristics at different time points of an L-COSY spectrum are derived here. Prior to the first slice-selective 90° RF pulse, the spin-state is represented by:

$$\sigma_0 \propto I_z \qquad [2.1]$$

where I is the spin under consideration and S is its J-coupled partner. After the rotation by the first 90° RF pulse, the spin-state is explained by:

$$\sigma_1 \propto -I_y. \qquad [2.2]$$

After an evolution during the interval of 2Δ, the spins evolve under the influence of J-coupling, but the chemical shift will be refocused resulting in an echo characterized by:

$$\sigma_2' \propto I_y \cos(2\pi J\Delta) - 2I_x S_z \sin(2\pi J\Delta). \qquad [2.3]$$

The evolution due to both chemical shift ($\omega_1^{(I)}$) and J-coupling with its coupled partner during the t_1 evolution is considered here.

$$\begin{aligned}\sigma_2 \propto [&I_y \cos(\omega_1^{(I)} t_1)\cos(\pi J t_1) - 2I_x S_z \cos(\omega_1^{(I)} t_1)\sin(\pi J t_1) \\ &- I_x \sin(\omega_1^{(I)} t_1)\cos(\pi J t_1) - 2I_y S_z \sin(\omega_1^{(I)} t_1)\sin(\pi J t_1)] \\ &\times \cos(2\pi J\Delta) - [2I_x S_z \cos(\omega_1^{(I)} t_1)\cos(\pi J t_1) \\ &+ I_y \cos(\omega_1^{(I)} t_1)\sin(\pi J t_1) + 2I_y S_z \sin(\omega_1^{(I)} t_1)\cos(\pi J t_1) \\ &- I_x \sin(\omega_1^{(I)} t_1)\sin(\pi J t_1)]\sin(2\pi J\Delta). \qquad [2.4]\end{aligned}$$

Let us define the following to simplify the Eq. [2.4]:

$$A = \cos(\omega_1{}^{(I)}t_1)\cos(\pi J t_1) \quad [2.4a]$$

$$B = \cos(\omega_1{}^{(I)}t_1)\sin(\pi J t_1) \quad [2.4b]$$

$$C = \sin(\omega_1{}^{(I)}t_1)\cos(\pi J t_1) \quad [2.4c]$$

$$D = \sin(\omega_1{}^{(I)}t_1)\sin(\pi J t_1) \quad [2.4d]$$

$$\sigma_2 \propto \{AI_y - B2I_xS_z - CI_x - D2I_yS_z\}\cos(2\pi J\Delta) - \{A2I_xS_z + BI_y + C2I_yS_z - DI_x\}\sin(2\pi J\Delta). \quad [2.5]$$

A second pair of B_0 gradient crusher pulses was transmitted around the last slice-selective 90° RF pulse. After an evolution during the first set of crusher gradient pulses, the spin state is represented by:

$$\begin{aligned}\sigma_3 \propto \{&AI_y\cos\theta_1 - AI_x\sin\theta_1 - CI_x\cos\theta_1 - CI_y\sin\theta_1 \\ &- B2I_xS_z\cos\theta_1 - B2I_yS_z\sin\theta_1 - D2I_yS_z\cos\theta_1 \\ &+ D2I_xS_z\sin\theta_1\}\cos(2\pi J\Delta) - \{BI_y\cos\theta_1 - BI_x\sin\theta_1 \\ &- DI_x\cos\theta_1 - DI_y\sin\theta_1 + A2I_xS_z\cos\theta_1 + A2I_yS_z\sin\theta_1 \\ &+ C2I_yS_z\cos\theta_1 - C2I_xS_z\sin\theta_1\}\sin(2\pi J\Delta). \quad [2.6]\end{aligned}$$

The spin state after the last 90° RF pulse rotation:

$$\begin{aligned}\sigma_4 \propto \{&AI_z\cos\theta_1 - AI_x\sin\theta_1 - CI_x\cos\theta_1 - CI_z\sin\theta_1 \\ &+ B2I_xS_y\cos\theta_1 + B2I_zS_y\sin\theta_1 + D2I_zS_y\cos\theta_1 \\ &- D2I_xS_y\sin\theta_1\}\cos(2\pi J\Delta) - \{BI_z\cos\theta_1 - BI_x\sin\theta_1 \\ &- DI_x\cos\theta_1 - DI_z\sin\theta_1 - A2I_xS_y\cos\theta_1 - A2I_zS_y\sin\theta_1 \\ &- C2I_zS_y\cos\theta_1 + C2I_xS_y\sin\theta_1\}\sin(2\pi J\Delta). \quad [2.7]\end{aligned}$$

At this point, evolution of I_z and $2I_xS_y$ will be excluded since there will be no observable signal. The spin state after an evolution during the last set of B_0 gradient crushers (θ_2):

$$\begin{aligned}\sigma_5 \propto &-0.5\cos(2\pi J\Delta)[I_y\cos(\omega_1{}^{(I)}t_1)\cos(\pi J t_1) \\ &+ I_x\sin(\omega_1{}^{(I)}t_1)\cos(\pi J t_1) + 2I_zS_x\cos(\omega_1{}^{(I)}t_1)\sin(\pi J t_1) \\ &- 2I_zS_y\sin(\omega_1{}^{(I)}t_1)\sin(\pi J t_1)] + 0.5\sin(2\pi J\Delta) \\ &\times [I_y\cos(\omega_1{}^{(I)}t_1)\sin(\pi J t_1) + I_x\sin(\omega_1{}^{(I)}t_1)\sin(\pi J t_1) \\ &- 2I_zS_x\cos\times(\omega_1{}^{(I)}t_1)\cos(\pi J t_1) + 2I_zS_y\sin(\omega_1{}^{(I)}t_1)\cos(\pi J t_1)]. \quad [2.8]\end{aligned}$$

Equation [2.8] was calculated under the assumption that the gradient crushers are balanced ($\theta_1 = \theta_2$) and also using Eq. [1.7]. The phase factors, θ_1 and θ_2, are defined in Eqs. [1.4a] and [1.6a]. It is also evident from Eq. [2.8] that the coherence transfer from spin *I* to *S* is characterized by $2I_zS_x$ and $2I_zS_y$. A similar equation was also calculated for *S* spin resulting in a coherence transfer to *I* spin. The 2D signal acquired after the last crusher gradients is given by:

$$s(t_1, t_2) = \mathrm{Tr}\{(I_x)\sigma_5\}\exp(-i\omega_2{}^{(I)}t_2)\exp(-t_1/T_2) \times \exp(-t_2/T_2)[1 - \exp(-TR/T_1)]. \quad [2.9]$$

A double Fourier transformation along both t_1 and t_2 axes will result in a 2D MR spectrum as a function of two frequency variables (F_1, F_2) described by:

$$S(F_1, F_2) = \int\int s(t_1, t_2)\, dt_1\, dt_2. \quad [2.10]$$

Aue et al. (37) reported that the diagonal peaks were dispersive, whereas the cross-peaks were absorptive when two hard 90° RF pulses were used to acquire the COSY spectrum. One drawback of including the gradient pulses is due to the mixed line shapes in the 2D NMR spectra (38). Equation [2.8] clearly indicates that both the diagonal and cross-peaks of an L-COSY spectrum have mixed phases along the F_1 axis. In contrast to the amplitude modulation in conventional COSY, the phase modulation in L-COSY is caused by the evolution during the B_0 gradient pulse before the last 90° RF pulse (38). Pure phase L-COSY spectrum can be recorded using a quadrature detection method along the F_1 axis described by Doddrell and co-workers (38) that will require two separate P- and N-type spectral acquisition and recombination of the two datasets. Relaxation during the gradient pulses before the last 90° RF pulse will cause further losses in signal intensities.

RESULTS

The correctness of the volume localization part of the CABINET sequence was ascertained by recording a 3 × 3 × 3 cm^3 voxel image recorded using the following parameters: TR/TE = 1000/30 ms, FOV = 16 cm, NEX = 1, and 256 × 128. A 27 ml 2D L-COSY spectrum of a GE MRS phantom with the cerebral metabolites at physiological concentrations and at pH = 7.2 is shown in Fig. 2. The time-domain raw signal had 1024 complex points along the t_2 and 128 points along the t_1 axes. A total of eight averages was acquired for every Δt_1 which resulted in a total duration of 35 min for signal acquisition. The 2D raw data was apodized with squared sine bell filters (with a 90° phase shift along the t_2 dimension only) and zero filled to a matrix size of 2048 × 256 prior to complex Fourier transformation along both dimensions. The resulting 2D spectrum was displayed in the magnitude mode. The pattern of the diagonal peaks at $F_2 = F_1$ resembled the conventional 1D spectral resonances, whereas the cross-peaks due to J-coupling between various protons of metabolites were asymmetrically disposed on both sides of the diagonal peaks. Shown in Fig. 3 are 2D COSY spectra of six metabolites, namely, NAA, glutamine, glutamate, myo-inositol, creatine, and choline recorded individually under identical experimental conditions. These spectra were used to assign some of the 2D spectral peaks shown in Fig. 2. The 2D cross-peaks were predominantly monitored in the following locations: 1) NAA: (4.35 ppm, 2.5 ppm) and (2.5 ppm, 4.35 ppm), 2) Glu: (3.75 ppm, 2.25 ppm) and (2.25 ppm, 3.75 ppm), 3) lactate: (4.1 ppm, 1.25 ppm) and (1.25 ppm, 4.1 ppm), 4) Cr: (3.9 ppm, 3.0 ppm) and

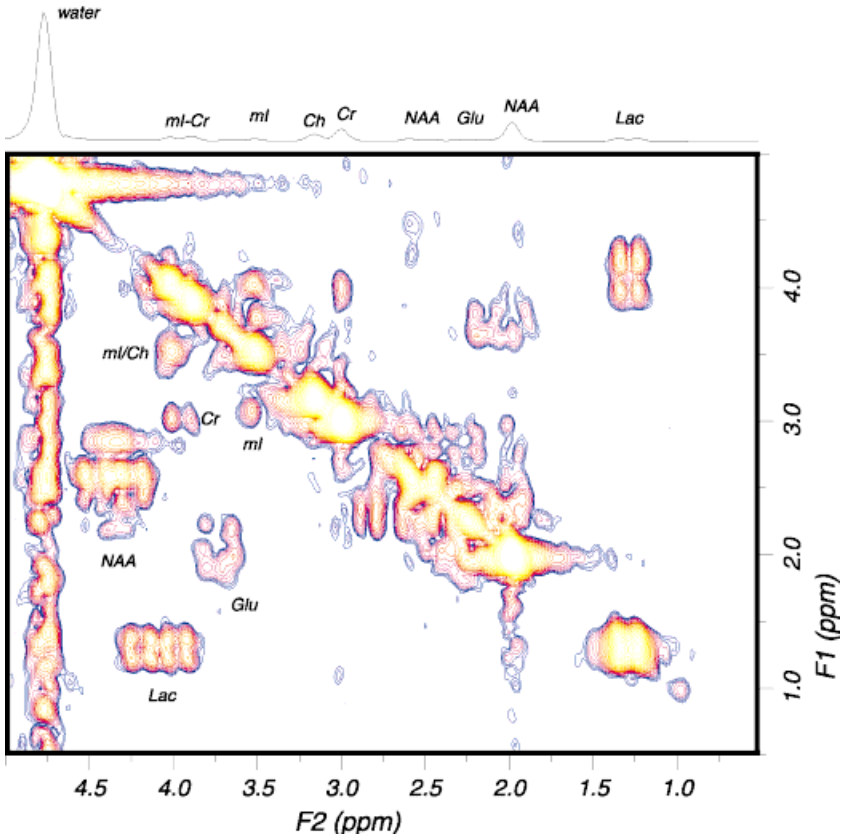

FIG. 2. 2D L-COSY MR spectrum of a brain phantom using 27 ml. 1024 complex points were used to sample the F_2 dimension and 128 Δt_1 increments with eight averages per increment along the F_1 dimension. The 2D raw data were zero-filled to 256 and 2048 along F_1 and F_2 axes and displayed in the magnitude mode.

(3.0 ppm, 3.9 ppm), and 5) mI: (4.0 ppm, 3.54 ppm), (3.54 ppm, 3.1 ppm), (3.1 ppm, 3.54 ppm), and (3.54 ppm, 4.0 ppm).

The cerebral L-COSY spectra recorded from a 27 ml voxel localized in a 25-year-old healthy volunteer are shown in Fig. 5. The MRS voxel was placed in the prefrontal gray/white matter, as shown in Fig. 4. With eight averages per Δt_1, the 2D spectra shown in Fig. 5 were acquired using a) 40 Δt_1 and b) 128 Δt_1 increments that resulted in a total duration of 11 min and 35 min, respectively. As expected, both diagonal and cross-peaks were severely broadened along the F_1 dimension when 40 increments were used to sample the second dimension. However, the cross-peaks due to NAA and glutamate/glutamine (Glx) were distinctly visible. The cross-peaks due to aspartate and creatine were also present with a limited dispersion. The reported frontal gray matter metabolite concentrations of NAA, Glx, mI, and Ch are 8 mM, 12 mM, 4 mM, and 1.3 mM, respectively (39). The auto-cross-peaks and the cross-peaks between protons which have smaller chemical shift dispersion were severely overlapping with the dominant diagonal peaks. Improved resolution of the cross-peaks and diagonal peaks was obtained with 128 Δt_1, as shown in Fig. 5b. In particular, the cross-peaks due to myo-inositol were well resolved in Fig. 5b. It was also evident that the cross-peak intensities of metabolites with short T_2 such as Glx decreased with higher Δt_1.

A 2D L-COSY spectrum, shown in Fig. 6b, was recorded in the occipital gray/white matter region of a 22-year-old healthy volunteer. The MRS voxel location is shown in Fig. 6a. The parameters used to record the L-COSY spectrum were: $3 \times 3 \times 3$ ml, 1024 and 64 complex points along t_2 and t_1 dimensions, NEX = $16/\Delta t_1$, a total duration of 35 min for 2D acquisition. The 2D spectrum had better sensitivity than Fig. 5b, but the peaks were broadened along F_1 due to fewer increments.

DISCUSSION

In the conventional 1D ^{1}H MR spectra, mostly the dominant singlets due to NAA (2 ppm), Cr (3 ppm), and Ch (3.15 ppm) were used when calculating the metabolite ratios and absolute metabolite concentrations (1–12). The spectral peaks due to methyl, methylene, and methine of NAA, Glx, GABA, Asp, Glc, N-acetyl aspartyl glutamate (NAAG), and other metabolites severely overlap, especially in the region of 2–4 ppm (40,41). Spectral overlap of macromolecules and glutathione (GSH) with the methyl resonances of Cr at 3 ppm, and that of NAAG and glutamate/glutamine with the methyl resonance of NAA at 2 ppm, have also been reported (40–42). T_2-weighted spectra using long TEs and spectral editing sequences have been used to differentiate a selected metabolite from the overlapping spectral peaks (1,13–17). Unlike the spectral editing techniques which target one metabolite at a time, 2D MRS can unambiguously resolve many overlapping peaks nonselectively, as demonstrated by Ernst and coworkers (22) two decades ago. In addition, better dispersion of several metabolite peaks and improved spectral assignment make the proposed technique more attractive. In conventional 1D MRS, the individual phase of the spectral peaks is influenced by the residual water tail. Due to

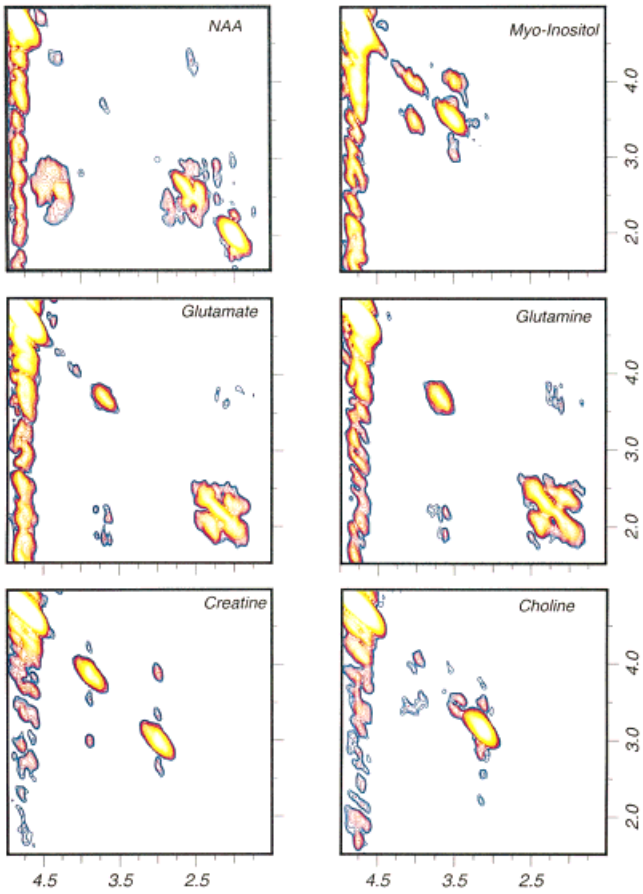

FIG. 3. 2D L-COSY spectra of six different metabolite phantoms using the same parameters for acquisition and postprocessing as used for Fig. 2.

the added second dimension, this was not the case in a 2D L-COSY spectrum. Unlike the 1D MR spectra, the 2D L-COSY spectral peaks were not dependent on the overall baseline of the spectrum.

There were two distinct singlets due to creatine/phosphocreatine (3 ppm and 3.9 ppm) in the conventional 1D spectrum. The respective methyl and methylene protons of Cr/PCr do have measurable J-coupling which are separated by a long range (four-bond) coupling of 0.25 Hz. In the L-COSY spectrum, there were two strong diagonal peaks at (F_1 = 3.0 ppm) and (F_1 = 3.9 ppm), and weak cross-peaks at (F_2 = 3.9 ppm, F_1 = 3.0 ppm) and (F_2 = 3.0 ppm, F_1 = 3.9 ppm), mainly due to Cr/PCr in conformity with the previous reports (30,32). A simulated 1.5T L-COSY spectrum of Cr using a GAMMA library clearly showed the 2D cross-peaks (36). In addition to the major metabolites (NAA, Glx, mI, Cr) at cerebral concentrations greater than 5 mM, the 2D cross-peaks due to metabolites at concentration in the range of 1–3 mM were also identified, as discussed below.

Unequivocal detection of free aspartate moiety whose concentration is approximately 1.5 mM (39–41), is difficult even with the 1D spectral editing techniques due to a small chemical shift difference between the methylene and methine protons. The 2D L-COSY spectra of brain had the cross-peaks due to aspartate. There were two cross-peaks, between the methylene resonances centered at (F_2 = 3.8 ppm, F_1 = 2.85 ppm) and (F_2 = 2.85 ppm, F_1 = 3.8 ppm), probably due to aspartate. A concentration of 2 mM has been reported for GSH (41,42). The cross-peaks between the cysteinyl protons of GSH at F_2 = 4.5 ppm and F_1 = 2.95 ppm were indistinguishable from the dominant t_1 ridge of water in the L-COSY spectrum, but the presence of cross-peaks was confirmed whenever the water suppression was excellent. The 2D cross-peaks of GABA were clearly identified at (F_2 = 3.0 ppm, F_1 = 1.9 ppm) and (F_2 = 1.9 ppm, F_1 = 3.0 ppm) when 16 or more averages per Δt_1 were acquired.

In the case of choline, the three N-methyl protons resonate at 3.15 ppm as a singlet in 1D MR spectroscopy due to the magnetic equivalence of the nine protons. The methyl protons lead to a strong diagonal peak (F_1 = 3.15 ppm) in the 2D L-COSY spectrum. The methylene protons of Ch resonating at 3.5 and 4 ppm, respectively, are J-coupled. They had cross-peaks at (F_2 = 3.5 ppm, F_1 = 4.0 ppm) and (F_2 = 4.0 ppm, F_1 = 3.5 ppm), which were overlapping with one of the cross-peak pairs of myo-inositol. A singlet due to glycine has been assigned at 3.5 ppm overlapping with one of the mI peaks (41). Hence, the 2D cross-peaks at (F_2 = 3.54 ppm, F_1 = 3.1 ppm) and (F_2 = 3.1 ppm, F_1 = 3.54 ppm) were unambiguously assigned to mI. Even though the aromatic resonance of glucose (Glc) has been detected at high field strength (43), we were unable to resolve a cross-peak between this resonance and the high field multiplets. Peres et al. (44) were able to identify these peaks after glucose loading of the rat brain. The cross-peaks between 3.4 ppm and 3.7 ppm due to Glc, and between 3.15 ppm and 3.4 ppm due to taurine (Tau), were close to the diagonal peaks. The 2D L-COSY cross-peaks

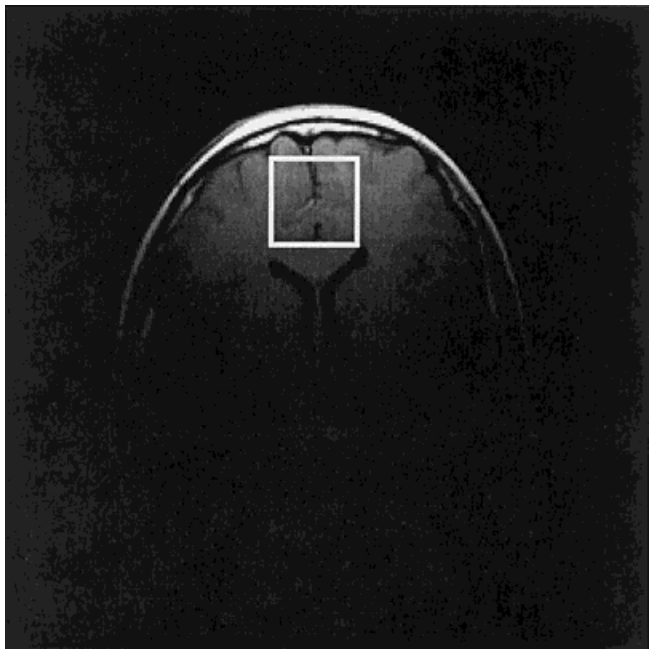

FIG. 4. Axial MR image of a 25-year-old healthy control. TR/TE = 500 ms / 14ms, FOV = 24 cm, matrix size of 256 × 128, and NEX = 1. A voxel size of 27 ml was used in the prefrontal gray/white matter region.

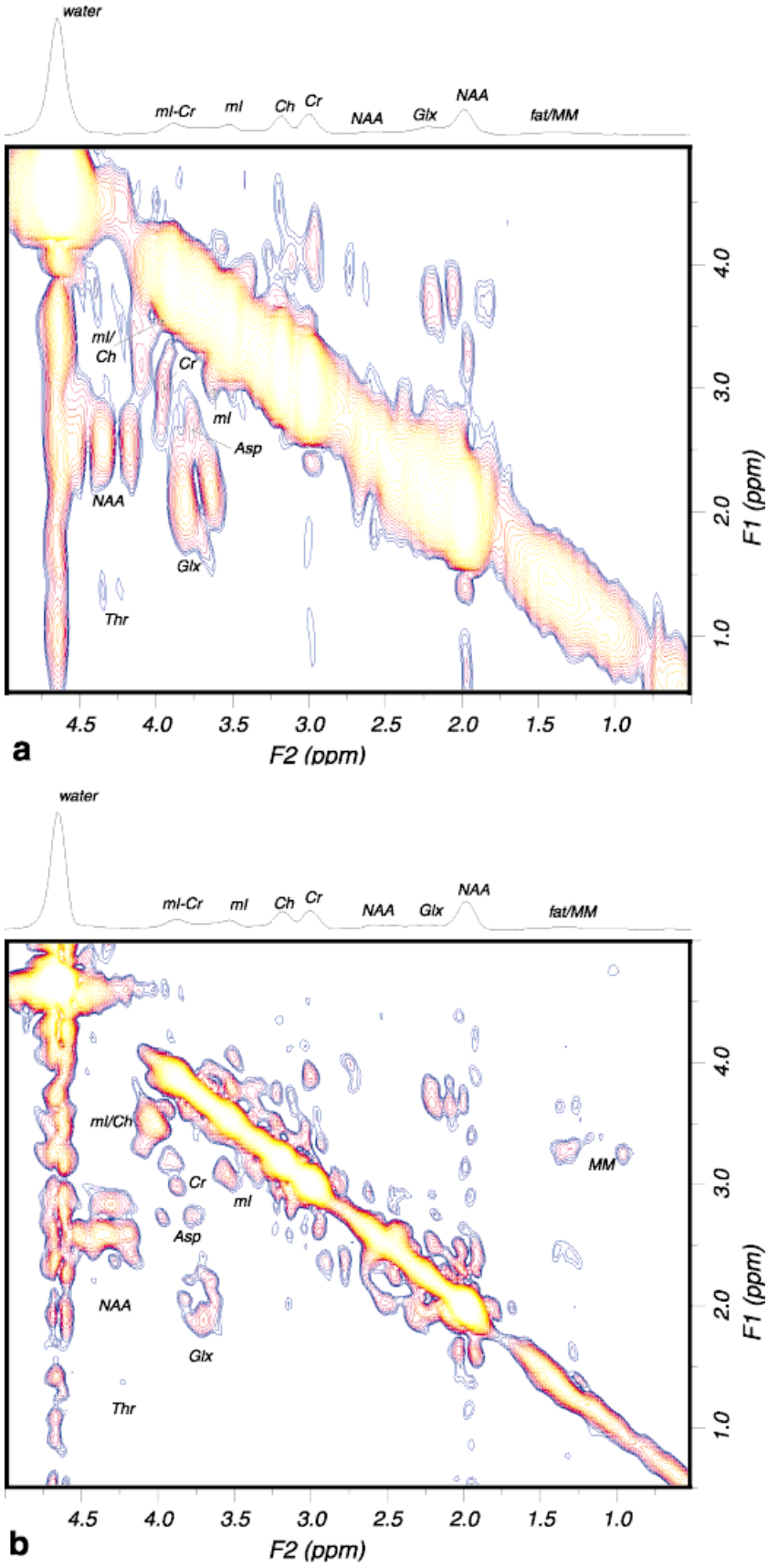

FIG. 5. 2D L-COSY spectra recorded in the prefrontal gray/white matter area. 1024 complex points were used to sample the F_2 dimension. 40 Δt_1 (**a**) and 128 Δt_1 (**b**) increments were used to sample the second dimension (F_1) with eight averages per increment. The 2D raw data were zero-filled to 128 in **a** and 256 in **b** along the F_1, and to 2048 along the F_2 axes.

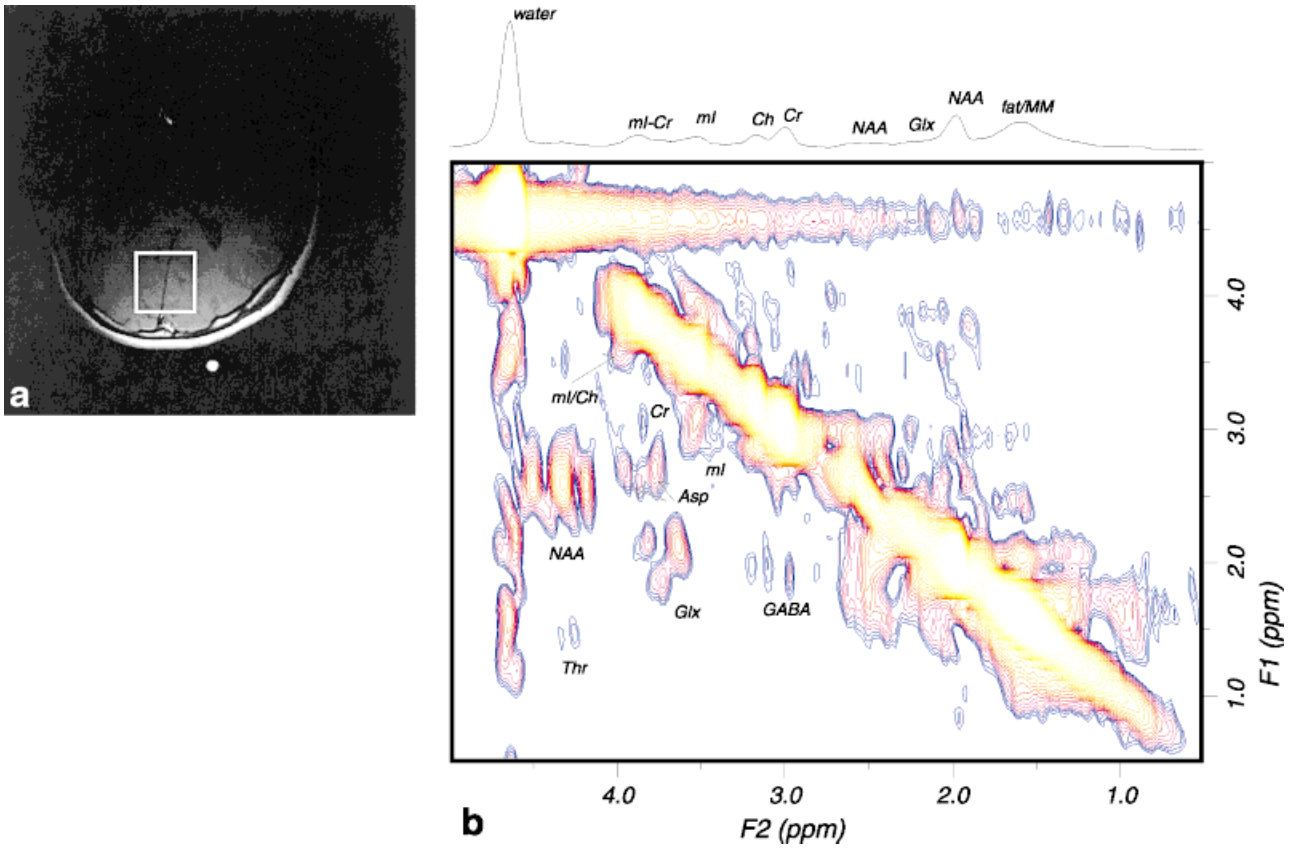

FIG. 6. **a:** Axial MRI of a 22-year-old healthy control with the MRS voxel location shown in the occipital gray/white matter area (27 ml). **b:** The corresponding 2D L-COSY spectrum. 1024 complex points were used to sample the F_2 dimension and 64 Δt_1 increments with 16 averages per increment along the F_1 dimension.

due to Glc and Tau were not clearly visible when fewer numbers of t_1 increments were used (40 Δt_1), but these cross-peaks were visible when 128 Δt_1 were used, as shown in Fig. 5b. There were only diagonal peaks in the region of 6–8 ppm, which probably represent exchangeable protons of cytosolic proteins (NAA, Glx, etc.) and aromatic protons of adenosine nucleotides (41).

As reported in the cerebral spectra of animal models (27,45), some of those connectivities between the protons of macromolecules were also identified in the L-COSY spectra at the following locations when larger number of averages/Δt_1 were used: (F_2 = 3.3 ppm, F_1 = 1.3 ppm), (F_2 = 1.9 ppm, F_1 = 1.0 ppm), (F_2 = 2.0 ppm, F_1 = 0.9 ppm), and (F_2 = 1.3 ppm, F_1 = 3.3 ppm). These resonances could be possibly due to thymosin, valine, leucine, etc., previously reported as M1–M7 resonances (14,45). There were also weak cross-peaks at (F_2 = 4.3 ppm, F_1 = 1.25 ppm) and (F_2 = 4.3 ppm, F_1 = 3.7 ppm) due to threonine and around (F_2 = 4 ppm, F_1 = 1.2 ppm) due to lactate/alanine, as reported by Behar and Ogino (27). Detection of threonine whose concentration is approximately 0.3 mM (41) using a voxel size of 27 ml clearly demonstrates the superior sensitivity of the proposed L-COSY technique.

The superior feature of the proposed L-COSY sequence compared to the previously published sequences is that the volume localization and the coherence transfer for COSY were simultaneously achieved using the last slice-selective RF pulse without adding more RF or gradient pulses (23–27). In contrast, volume localization and coherence transfer were enabled serially in a 2D COSY sequence proposed by Doddrell and co-workers (30). Due to the severe loss of signal in this sequence, a larger voxel size of 240 ml ($5 \times 6 \times 8$ cm^3) and a long acquisition time of 1 h and 42 min were required for a 2D COSY spectrum. The localized COSY sequence proposed by Cohen et al. (25) used two hard 90° RF pulses separated by the phase-encoding gradients. A major problem with this sequence is in adjusting the B_0 homogeneity. Blackband et al. (26) used the SLO-COSY sequence in which two slice-selective 90° RF pulses were used and a possibility of extending to a volume localization with a third slice-selective RF pulse was also mentioned. A double-quantum (DQ) filtered COSY of human muscle demonstrated by Kreis and Boesch used five RF pulses and had worse signal losses (29). CT-PRESS sequence proposed by Dreher and Leibfritz (31) had a fourth RF pulse in addition to a volume localizing PRESS sequence. 2D diagonal peaks of rat brain with homonuclear decoupling had better sensitivity. However, there was only a limited spectral dispersion as the multiplicity of the entire set of metabolite peaks was collapsed and the spectra were presented in the conventional 1D mode. Even though the 2D JPRESS sequence was more sensitive than the L-COSY sequence, the limited spectral

resolution along the second axis (F_1) resulted in an overcrowded 2D JPRESS spectrum compounded by the unavoidable strong coupling effects at 1.5 T field strength (19).

The cross-peaks were asymmetric with respect to the diagonal. The asymmetry was especially more severe in the upper diagonal cross-peaks of NAA at (F_2 = 2.5 ppm, F_1 = 4.35 ppm). Since the methine and a few methylene proton resonances appear close to the water peak, a water suppression RF pulse most likely saturated these resonances that lie within the RF bandwidth. A complete presence of the upper diagonal cross-peaks of NAA was confirmed by two independent experimental observations: 1) A 2D L-COSY spectrum of NAA in D_2O was recorded using the same pulse sequence without water suppression, and 2) A 2D L-COSY spectrum of NAA in water was recorded after deliberately adding an offset of 30–60 Hz to the carrier frequency. Even though water suppression was worse, the upper diagonal NAA cross-peaks were still observable. Theoretical 2D COSY spectra simulated using GAMMA library (36) without water suppression revealed additional sources of asymmetry contributed by the following factors (46): i) poor resolution along the F_1 dimension, and ii) J-evolution during the first spin-echo.

The twisted line-shape of the L-COSY peaks and the strong coupling effect (47) inherent at 1.5 T field strength are advantageous for human brain 2D MRS, since a poor resolution along the t_1 dimension does not lead to cancellation of the cross-peaks, as demonstrated in Fig. 5a for NAA, Glx, and mI. The mixed phase characteristics of the diagonal peaks were a major concern in identifying these cross-peaks that appear very close to the diagonal. In particular, the cross-peaks due to mI were resolvable only when 64 and 128 Δt_1 increments were used. However, this can be overcome by recording the P- and N-type L-COSY spectra separately (37). Pure phase 2D spectra and higher field strength could alleviate this problem (37,43). A second problem was due to the so-called "t_1-ridges" (22). This could be due to the instability of the RF amplifier and the subject moving during the acquisition of a 2D scan. In our pilot study with 15 healthy controls, the quality of the 2D L-COSY spectral peaks was hampered due to t_1-ridges only in two cases, mainly due to the subject's motion.

CONCLUSIONS

In addition to the commonly used STEAM and PRESS sequences for localized in vivo MRS, a new volume localization sequence, CABINET, the 1D analog of L-COSY, has been implemented on a whole-body 1.5 T MRI/MRS scanner. Similar to the PRESS sequence, the proposed sequence is also double echo-based, where the first spin echo originates from the first two slice-selective 90° and 180° RF pulses and the second coherence transfer echo from the last slice-selective 90° RF pulse. The volume localization efficiency of the proposed sequence was only 50%.

The 2D L-COSY spectra of a brain phantom as well as human brain in vivo showed asymmetric cross-peaks for J-coupled metabolites. Localized 2D COSY spectra have been recorded in the human frontal and occipital gray/white matter regions using a minimal number of RF pulses for both volume localization and coherence transfer. The 2D J-cross-peaks between the methine, methyl, and methylene protons of NAA, glutamate/glutamine, myo-inositol, creatine, aspartate, threonine/lactate, GABA, and macromolecules have been recorded. Even though the localization efficiency was only 50% with L-COSY/CABINET compared to the 2D JPRESS sequence (19–21), the 2D cross-peaks in an L-COSY spectrum had better dispersion of the J-cross-peaks between various protons of cerebral metabolites. The 2D J-cross-peaks enabled an unambiguous assignment of methylene protons of NAA, Glx, aspartate, mI, and threonine. The 2D L-COSY spectra recorded in the prefrontal as well as the occipitoparietal gray/white matter regions in a total of 15 healthy controls reveal the reliability of the technique in different regions of human brain. The superior sensitivity of the proposed 2D L-COSY technique is confirmed by detection of threonine and other metabolites with lower concentrations.

Due to the increased signal-to-noise compared to a head MRI coil, a 3" surface coil was used for reception in combination with the body coil transmission. The 2D L-COSY spectra recorded at smaller volumes (8 or 18 ml) showed the 2D cross-peaks only due to the most abundant cerebral metabolites, NAA, Glx, and mI. The 2D cross-peaks of glutamate were indistinguishable from that of glutamine at the 1.5 T magnetic field strength; however, high field MR scanners (>3 T) would facilitate such differentiation. The 2D L-COSY spectra using a voxel size of as small as 1 cm^3 have also been recorded in human breast cancer in vivo recently (48). With the increased spectral resolution enabled by the added second dimension, we expect the absolute quantitation of several metabolites using the L-COSY spectra to be more accurate than the conventional 1D spectra.

ACKNOWLEDGMENTS

The authors thank Lawrence Ryner Ph.D. and Yong Ke Ph.D. for help in the early phase of this project, and Prof. C. Griesinger, Dr. V.V. Krishnan, Prof. R. Brueschweiler, Dr. S. Sendhil Velan, Prof. G. Bodenhausen, Dr. O.W. Sorensen, Dr. N. Mueller, and Prof. Anil Kumar for scientific discussions. We thank Drs. Scott Smith, Andrew Maudsley, Wolfgang Dreher and Karl Young for providing the GAMMA library and related macros and Dr. S. Banakar for assistance with simulation.

REFERENCES

1. Hanstock CC, Rothman DL, Prichard JW, Jue T, Shulman RG. Spatially localized NMR spectra of metabolites in the human brain. Proc Natl Acad Sci USA 1988;85:1821–1825.
2. Braun H, Frahm J, Gyngell ML, Merboldt KD, Hanicke W, Suter R. Cerebral metabolism in man after acute stroke: new observation using localized proton NMR Spectroscopy. Magn Reson Med 1989;9:126–131.
3. Kuzniecky R, Hetherington H, Pan J, Hugg J, Palmer C, Gilliam F, Faught E, Morawetz R. Proton spectroscopic imaging at 4.1 Tesla in patients with malformations of cortical development and epilepsy. Neurology 1997;48:1018–1024.
4. Barberi EA, Gai JS, Rutt BK, Menon RS. A transmit-only/receive only (TORO) system for high field MRI/MRS applications. Magn Reson Med 2000;43:284–289.
5. Kreis R, Ross BD, Farrow N, Ackerman Z. Metabolic disorders of the brain in chronic hepatic encephalopathy detected with ^1H MR spectroscopy. Radiology 1992;182:9–27.

6. Chang L, Ernst T, Yee ML, Walot I, Singer E. Cerebral metabolite abnormalities correlate with clinical severity of HIV-1 cognitive motor complex. Neurology 1999;52:100–108.
7. Thomas MA, Huda A, Guze B, Curran J, Bugbee M, Fairbanks L, Ke Y, Oshiro T, Martin P, Fawzy F. Cerebral ^{1}H MR Spectroscopy and Neuropsychological status of patients with hepatic encephalopathy. Am J Roentgenol 1998;171:1123–1130.
8. Thomas MA, Ke Y, Levitt J, Caplan R, Curran J, Asarnow R, McCracken J. Preliminary study of frontal lobe ^{1}H MR spectroscopy in childhood-onset schizophrenia. J Magn Reson Imag 1998;8:841–846.
9. Narayana PA, Doyle TJ, Lai D, Wolinsky JS. Serial proton magnetic resonance spectroscopic imaging, contrast-enhanced magnetic resonance imaging, and quantitative lesion volumetry in multiple sclerosis. Ann Neurol 1998;43:56–71.
10. Haseler LJ, Sibbitt WL, Mojtahedzadeh HN, Reddy S, Agarwal VP, McCarthy DM. Proton MR spectroscopic measurement of neurometabolites in HE during oral lactulose therapy. Am J Roentgenology 1998;19: 1681–1686.
11. Michelis T, Merboldt KD, Bruhn H, Hanicke W, Frahm J. Absolute concentrations of metabolites in the adult human brain in vivo: quantification of localized proton MR spectra. Radiology 1993;187:219–227.
12. Ernst T, Kreis R, Ross BD. Absolute quantitation of water and metabolites in the human brain. I. Compartments and water. J Magn Reson 1993;B102:1–8.
13. Rothman DL, Petroff OAC, Behar KL, Mattson RH. Localized ^{1}H NMR measurements of γ-aminobutyric acid in human brain in vivo. Proc Natl Acad Sci USA 1993;90:5662–5666.
14. Behar KL, Rothman DL, Spencer DD, Petroff OAC. Analysis of macromolecule resonances in ^{1}H NMR spectra of human brain. Magn Reson Med 1994;32:294–302.
15. Keltner JR, Wald LL, Frederick BdB, Renshaw PF. In vivo detection of GABA in human brain using a localized double-quantum filter technique. Magn Reson Med 1997;37:366–371.
16. Thomas MA, Hetherington HP, Meyerhoff DJ, Twieg D. Localized double quantum filtered NMR spectroscopy. J Magn Reson 1991;B93:485–496.
17. Wilman A, Allen P. In vivo NMR detection strategies for γ-aminobutyric acid, utilizing proton spectroscopy and coherence-pathway filtering with gradients. J Magn Reson 1993;B101:165–171.
18. Ryner LN, Sorenson JA, Thomas MA. 3D localized 2D NMR spectroscopy on an MRI scanner. J Magn Reson B 1995;107:126–137.
19. Ryner LN, Sorenson JA, Thomas MA. Localized 2D *J*-Resolved ^{1}H MR spectroscopy: strong coupling effects *in vitro* and *in vivo*. Magn Reson Imag 1995;13:853–869.
20. Thomas MA, Ryner LN, Mehta M, Turski P, Sorenson JA. Localized 2D J-resolved ^{1}H MR spectroscopy of human brain tumors *in vivo*. J Magn Reson Imag 1996;6:453–459.
21. Hurd RE, Gurr D, Sailasuta N. Proton spectroscopy without water suppression: the oversampled J-resolved experiment. Magn Reson Med 1998;40:343–347.
22. Ernst RR, Bodenhausen G, Wokaun A. Principles of NMR spectroscopy in one and two dimensions. Oxford: Oxford Publications; 1987.
23. McKinnon GC, Bosiger P. Localized double quantum filter and correlation spectroscopy experiments. Magn Reson Med 1988;6:334–343.
24. Haase A, Schuff N, Norris D, Leibfritz D. Localized COSY NMR spectroscopy. In: Proc of the 7th Annual Meeting SMRM, 1987. p 1051.
25. Cohen Y, Chang LH, Litt L, James TL. Spatially localized COSY spectra from a surface coil using phase-encoding magnetic field gradients. J Magn Reson 1989;85:203–208.
26. Blackband SJ, McGovern KA, McLennan IJ. Spatially localized two-dimensional spectroscopy. SLO-COSY and SLO-NOESY. J Magn Reson 1988;79:184–189.
27. Behar KL, Ogino T. Assignment of resonances in the ^{1}H spectrum of rat brain by two-dimensional shift correlated and J-resolved NMR spectroscopy. Magn Reson Med 1991;17:285–303.
28. de Graaf RA, Kranenburg AV, Nicolay K. Off-resonance metabolite magnetization transfer measurements on rat brain in situ. Magn Reson Med 1999;41:1136–1144.
29. Kreis R, Boesch C. Spatially localized, one- and two-dimensional NMR spectroscopy and in vivo application to human muscle. J Magn Reson 1996;B113:103–118.
30. Brereton IM, Galloway GJ, Rose SE, Doddrell DM. Localized two-dimensional shift correlated spectroscopy in humans at 2 Tesla. Magn Reson Med 1994;32:251–257.
31. Dreher W, Leibfritz D. Detection of homonuclear decoupled in vivo proton NMR spectra using constant time chemical shift encoding: CT-PRESS. Magn Reson Imag 1999;17:141–150.
32. Barrere B, Peres M, Gillet B, Mergui S, Beloeil JC, Seylaz J. 2D COSY ^{1}H NMR: a new tool for studying in situ brain metabolism in the living animal. FEBS 1990;264:198–202.
33. Berkowitz BA, Wolff SD, Balaban RS. Detection of metabolites in vivo using 2D proton homonuclear correlated spectroscopy. J Magn Reson 1988;79:547–553.
34. Webb P. Application of crafted pulses to *in vivo* spectroscopy. In: Proc 11th Annual Meeting SMRM,1992. p 2131.
35. Schirmer T, Auer DP. On the reliability of quantitative clinical magnetic resonance spectroscopy of the human brain. NMR Biomed 2000; 13:28–36.
36. Smith SA, Levante TO, Meier BH, Ernst RR. Computer simulations in magnetic resonance. An object oriented programming approach. J Magn Reson 1994;A106:75–105.
37. Aue WP, Bartholdi E, Ernst RR. Two-dimensional NMR spectroscopy. J Chem Phys 1976;64:2229–2246.
38. Brereton AM, Crozier S, Filed J, Doddrell DM. Quadrature detection in F_1 induced by pulsed field gradients. J Magn Reson 1991;93:54–62.
39. Pouwels PJW, Frahm J. Regional metabolite concentrations in human brain as determined by quantitative localized proton MRS. Magn Reson Med 1998;39:53–60.
40. Tyson RL, Sutherland GR. Labelling of N-acetylaspartate and N-acetylaspartylglutamate in rat neocortex, hippocampus and cerebellum from [1-^{13}C]glucose. Neurosci Lett 1998;251:181–184.
41. Govindaraju V, Young K, Maudsley AA. Proton NMR chemical shifts and coupling constatnts for brain metabolites. NMR Biomed 2000;13: 129–153.
42. Trabesinger AH, Webe OM, Duc Co, Boesiger P. Detection of glutathione in the human brain in vivo by means of double quantum coherence filtering. Magn Reson Med 1999;42:283–289.
43. Gruetter R, Weisdorf SA, Rajanayagan V, Terpstra M, Merkle H, Truwit CL, Garwood M, Nyberg SL, Ugurbil K. Resolution improvements in in vivo ^{1}H NMR spectra with increased magnetic field strength. J Magn Reson 1998;135:260–264.
44. Peres M, Fedeli O, Barrere B, Gillet B, Berenger G, Seylaz J, Beloeil JC. In vivo identification and monitoring of changes in rat brain glucose by two-dimensional shift-correlated ^{1}H NMR spectroscopy. Magn Reson Med 1992;27:356–361.
45. Kauppinen RA, Nissinen T, Karkkainen AM, Pirttila TR, Palvimo J, Kokko H, Williams SR. Detection of thymosin β4 in situ in a guinea pig cerebral cortex preparation using ^{1}H NMR spectroscopy. J Biol Chem 1992;267:9905–9910.
46. Griesinger C, Gemperle C, Sorensen OW, Ernst RR. Symmetry in coherence transfer: application to two-dimensional NMR. Mol Phys 1987; 62:295–332.
47. Thomas MA, Kumar A. Influence of strong coupling on two-dimensional spin-echo multiple-quantum NMR. Application to oriented spin system. J Magn Reson 1982;47:535–538.
48. Thomas MA, Binesh N, Yue K, DeBruhl N. Volume localized two-dimensional correlated MR spectroscopy of human breast cancer. J Magn Reson Imag 2001, in press.